

Article

Performance Analysis of a Grid-connected High Concentrating Photovoltaic System under Practical Operation Conditions

Zhe Mi ^{1,†}, Jikun Chen ^{2,*,†}, Nuofu Chen ^{1,3,*}, Yiming Bai ¹, Wenwang Wu ⁴, Rui Fu ¹ and Hu Liu ⁵

¹ State Key Laboratory of Alternate Electrical Power System with Renewable Energy Source, North China Electric Power University, Beijing 102206, China; mizhe@126.com (Z.M.); ymbai@ncepu.edu.cn (Y.B.); fuying815@126.com (R.F.)

² School of Materials Science and Engineering, University of Science and Technology Beijing, Beijing 100083, China

³ Yunnan Lincang Xinyuan Germanium Co. Ltd., Kunming 650503, China

⁴ State Key Laboratory of Automotive Safety and Energy, Tsinghua University, Beijing 100084, China; wenwang_wu@mail.tsinghua.edu.cn

⁵ Department of Mathematics and Physics, Shijiazhuang Tiedao University, Shijiazhuang 050043, China; liuhu@stdu.edu.cn

* Correspondence: jikunchen@ustb.edu.cn (J.C.); nfchen@ncepu.edu.cn (N.C.); Tel.: +86-10-6233-4143 (J.C.); +86-10-6177-2402 (N.C.)

† These authors contributed equally to this work.

Academic Editor: Wei-Chiang Hong

Received: 12 November 2015; Accepted: 4 February 2016; Published: 19 February 2016

Abstract: High concentrating photovoltaic (HCPV) is a promising technique for the practical commercial utilization of solar energy. However, the performance of a HCPV system is significantly influenced by environmental parameters such as solar direct normal irradiance (DNI) level and environmental temperature. This paper analyzes the performance of a 9 kW_p grid-connected HCPV system in Kunming (Yunnan, China), during practical field operations over an entire year, and discusses how the environmental parameters influence the performance from both the energy conversion and power inversion perspective. Large variations in the performance of the HCPV system have been observed for different months, due to the respective changes in the environmental parameters. The DNI level has been found to be a dominant parameter that mainly determines the amount of energy production as well as the performance ratio of the HCPV system. The environmental temperature and wind velocity have less influence on the system performance ratio than expected. Based on the performance of the present HCPV system, a quantified correlation between the output power and the direct normal irradiance has been derived, which provides guidelines for both the cogent application and the modeling of HCPV techniques for grid-connected power generation.

Keywords: HCPV system; performance ratio; efficiency; DNI; temperature

PACS: 88.40.hj

1. Introduction

Due to the fast development in industry and the growing population, the past 50 years have witnessed a dramatic increase in the consumption and cost of the fossil fuels remaining in limited amounts in the Earth's crust. Therefore, it is compulsory to develop suitable techniques to harvest

energy from renewable sources, which has aroused extensive interest since the middle of the last century all over the world. One of the most promising renewable energy techniques is photovoltaic (PV). PV devices (or solar cells) can realize the conversion of solar energy into electric power without emissions of CO₂ or chemical/radiation pollutants. Since 1960 or so, the PV technique was extensively applied in both industrial and spatial uses. As a result, the conversion efficiencies of PV modules have been improved significantly, while their costs were gradually reduced. By the year 2014, the global installed PV capacity has reached 177 GW in total [1]. Among all types of PV application, high concentrating photovoltaic (HCPV) techniques have been increasingly implemented, due to their high conversion efficiency and cost reduction potential [2–4]. In HCPV techniques, the sunlight is focused by optical concentrating devices (often Fresnel lenses for high concentrating) onto solar cell chips with much smaller area [5,6]. This effectively reduces the usage of the expensive solar cells and reduces the total cost. Usually, the high performance solar cells used for HCPV possess a multi-junction structure, where each junction possesses a distinguished band-gap. Therefore, it can more effectively absorb the sunlight with different wavelengths and realize a high conversion efficiency of more than 45% [7]. The levelised cost of electricity (LCoE) of a well-constructed HCPV power plant is expected to be similar to that of a conventional PV power plant using multiple-crystalline silicon solar cells [4,8].

However, the operation characteristics of a HCPV system under practical conditions are very different from that of non-concentrated PV systems [9]. The performance of the HCPV system is rather sensitive to the incident angle of the solar light and the HCPV can only efficiently make use of direct normal irradiation (DNI) [10,11]. In order to adjust the position of the solar panel according to the movement of the sun, a precise solar tracking system is required [12,13]. Therefore, the HCPV system possesses a more complex structure than conventional PV systems, which represents a challenge for the practical construction and field operation of HCPV power plants. Apart from the intensity of DNI, the distribution of the DNI can be also affected by the atmospheric conditions such as air density, moisture and aerosols [14,15]. The changes in the distribution of DNI are expected to result in mismatches in the photocurrent generated in the different junctions of the solar cell and reduces the performance [16,17]. Another parameter that is considered to largely influence the performance of HCPV systems is the environmental temperature, since an increase in temperature reduces the conversion efficiency of solar cells [18,19]. Due to these operational complexities, the practical performance of HCPV systems are less reported as compared to the conventional PV systems based on non-concentrating silicon solar cells. More investigations concerning how the complex environmental parameters influence the energy conversion and power inversion process of a HCPV system are still required.

In this paper, the practical field performance of a 9 kW_p grid-connected HCPV system located in Kunming has been investigated over an entire year. The direct current (DC) power before the inverter and the alternative current (AC) power after the inverter were measured as a function of time, along with the environmental parameters such as DNI and environmental temperature. The respective influences on final yield and performance ratio of the HCPV system by environmental parameters have been analyzed. Based on the experimental results, the influence of the environmental parameters to the performance of the HCPV system is discussed. A quantified correlation between energy production and solar direct normal irradiation has been derived in order to predict the power generation when installing similar HCPV power plant in the nearby regions based on the present technique.

2. Experimental

The 9 kW_p HCPV system was constructed in Kunming (Yunnan Province, China) in 2013. The site is located in Southwest China (24°47' N, 102°49' E) at an altitude of 1948 m above sea level and an annual global solar radiation around 1500–1600 kWh/m² [20]. The total installed capacity of the HCPV power plant is 100 kW_p. It consists altogether of 17 grid-connected HCPV generators, which includes five generators with 9 kW_p rated power and 12 generators with 4.5 kW_p rated power. One of the 9 kW_p generators has been used in the present investigation. Figure 1a shows its practical appearance. In brief, the HCPV system consists of 96 independent modules that are series/parallel

connected, as illustrated in Figure 1b. Each six modules are connected in series, forming altogether 16 strings and each eight strings are connected in parallel via a junction box, while the two junction boxes are connected to an inverter.

An individual module is comprised of 24 *III-V* multi-junction solar cell chips. In order to effectively absorb and convert the solar energy with broadly distributed wavelength, a three-junction of GaInP/GaInAs/Ge has been used for the solar cell, with TiO₂/SiO₂ anti-reflective coating on the surface. The active area of an individual solar cell chip is 30 mm² and the average conversion efficiency is 39.0% under 500 × concentration. The solar cell chip has been integrated with a set of solar concentrating devices which is used to concentrate the sun light, as illustrated by Figure 1c. The primary optical device is a Fresnel lens with 500 × geometric concentration intensity, while a core-shaped reflective tube is installed as a secondary optical device in order to enhance the homogeneity of the concentrated solar light spot on the the solar cell surface [21]. To form the module, 24 solar cells are connected in series, as illustrated by Figure 1d. The maximum DC output power of an individual module under standard test condition is around 93 W.

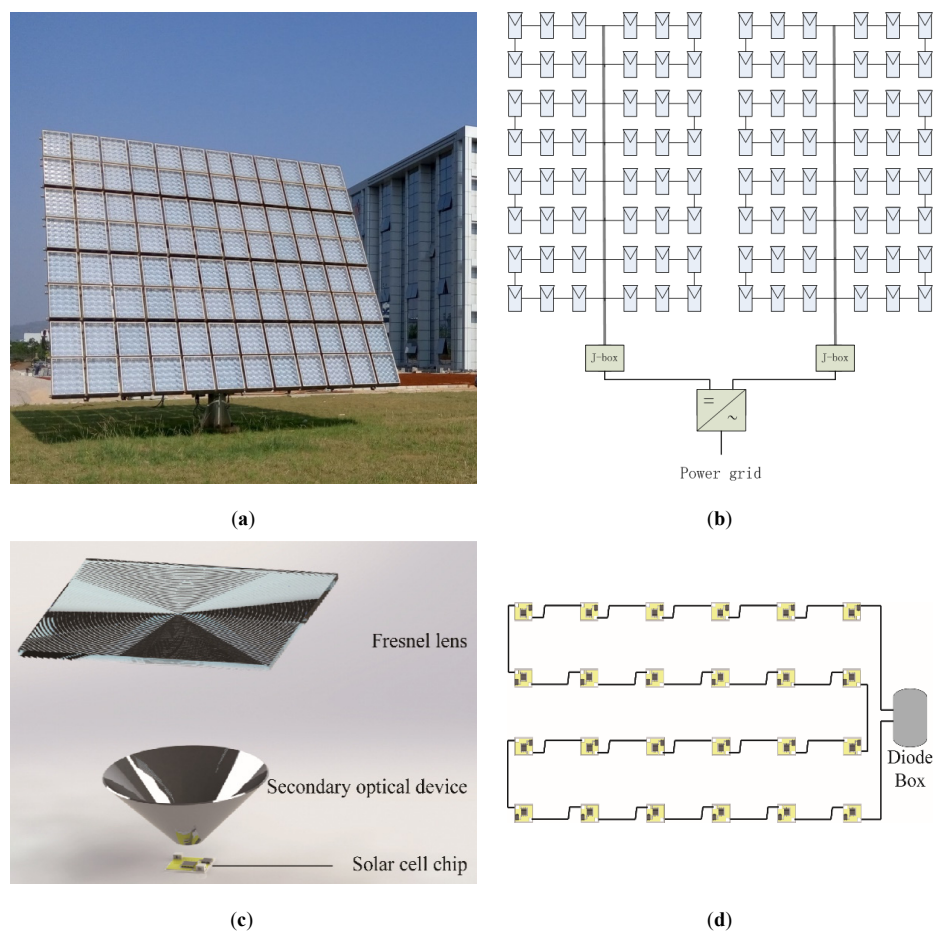


Figure 1. (a) Appearance of the 9 kW_p grid-connected HCPV system; (b) Illustration of electric connections of the HCPV modules; (c) Illustration of the individual solar cell chip combined with the optical concentrating device; (d) Illustration of solar cell connections in a module.

The 96 connected HCPV modules, which form an array, were mounted on the frame of a dual-axis solar tracker (Green Source Technology, Beijing, China) with the maximum tracking error of 0.2°. A 10 kW three-phase inverter (CEHE, Chizhou, China) was installed to transform the output power from DC to AC, which is further injected into a 380 V distribution network. The inverter requires no external power source and starts working after a delay time of 60 seconds after the input HCPV array

voltage exceeds 250 V. Otherwise, it will shut down when the input voltage goes below 250 V. In order to monitor the environmental parameters such as DNI, environmental temperature and wind velocity, a TRM-ZS2 type environment monitoring station (Sunshine Technology, Jinzhou, China) has been installed beside the HCPV system.

During the practical field operation, the input DC and output AC power (P_{DC} and P_{AC}) of the inverter were recorded as well as environment parameters as a function of time with a log interval of one minute from April to March 2015. The daily energy output from the inverter (E_{AC}) can be determined by integrating P_{AC} . The final yield of the HCPV system has been calculated by using E_{AC} divided by the rated PV capacity (P_{rated}), as $Y_F = (E_{AC}/P_{rated})$ [22–24], where P_{rated} for the present HCPV system has been characterized as 9 kW_p. The reference yield has been calculated as $Y_R = (H_{DNI}/H_R)$ [3,25], where H_{DNI} represents the direct normal irradiance while H_R represents the array reference irradiance (usually taken as 1 kW/m²). The performance ratio (PR) has been calculated by $P_R = (Y_F/Y_R)$ [23,24,26]. The instantaneous inverter efficiency has been calculated as $\eta_{inv} = P_{AC}/P_{DC} \times 100\%$ [27].

3. Results

The practical performances of the 9 kW_p grid-connected HCPV system have been monitored over the period between 1 April 2014 and 31 March 2015. An annual output AC power of 10,113 kWh was obtained in total. This indicates an energy production of 843 kWh per month and 27.7 kWh per day on average. The annual power consumption of the dual-axis solar tracker is around 43 kWh per year or 0.1 kWh per day, which only represent about 0.42% of the energy output of the HCPV system.

Figure 2 show the monthly average daily final yields and reference yields of the HCPV system as well as the performance ratio. The final yields and reference yields from January to May exceed the ones from June to December, which coincide with the division between the dry season (January to May) and wet season (June to December) in Kunming [28]. The highest final and reference yields, which reached 5.41 kWh/kW_p/day and 6.75 kWh/kW_p/day, respectively, were observed in March. The lowest ones were observed in June (final yield: 1.46 kWh/kW_p/day; reference yield: 1.77 kWh/kW_p/day). In general, a lower performance ratio has been observed for the wet season as compared to the dry season. As a more representative example, Figure A1 in the Appendix shows the measured direct normal irradiance as compared to the output AC power of the HCPV system in typical days for the dry season and wet season. In the dry season, the direct normal irradiance smoothly enhanced from the morning to the noon and afterwards reduced from noon to evening (see Figure A1a). Accordingly, the output power of the HCPV system shows a similar smooth variation (see Figure A1b).

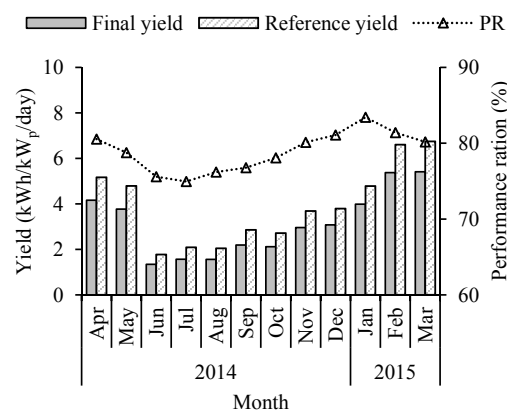


Figure 2. Monthly average daily value of final and reference yields and monthly performance ratio of the HCPV system.

This is in contrast to the situation observed for the wet season, where the direct normal irradiance is lower and fluctuates more frequently due to the shading by the heavy clouds (see Figure A1a).

As a result, the output energy is smaller and more fluctuated (see Figure A1b) as compared to the observations in dry season. When further comparing the performance of the HCPV systems in the present investigation to the previously reported PV power plants with different techniques in Table 1, the present HCPV system realizes an annually system efficiency (η) of 18.9% (using the measured DNI intensity as the reference), which values are comparable to the previous HCPV power plant reported in [16]. The annual averaged performance ratio of the present HCPV system has been calculated to be 79.7%, which value is lower than the HCPV system reported in [16]. The high system efficiency of the HCPV system is mainly because of the high conversion efficiency of the multi-junction solar cell chip (39%) as compared to the conventional crystalline silicon solar cell (<20%). In addition, the usage of solar tracking system in the HCPV system also benefits the reception of the incident solar light by the solar cells and improves the PV yields. Although possessing a high performance, the relatively high manufacture cost of the present HCPV system (around 2 \$/W_p) is still relatively higher than that of the commercialized PV systems based on crystalline silicon. Nevertheless, the installation cost of HCPV systems is expected to be greatly reduced when they are commercially produced, in which case the production line would be further improved and the production amount greatly increased.

Table 1. Performances of the present HCPV system located at Kunming as compared to previously reported PV/HCPV systems constructed in different locations (the DNI intensity is used for HCPV system when calculating the system efficiency).

Location	Latitude	PV type	P_{rate} (kW _p)	Final yield (kWh/kW _p /d)	PR (%)	System η (%)	Reference
Shanghai, China	31°12' N	Multi-Si	2.99	2.86	80.7	10.7	[26]
Gujarat, India	23.22° N	a-Si	500	3.99	70.8	6.1	[29]
Dublin, Ireland	53.4° N	Mono-/a-Si	1.72	2.41	81.5	12.6	[27]
Kuwait City	29°2' N	CIGS	85.05	4.5	70–85	11.1	[30]
Jaen, Spain	37°27' N	HCPV	1.35	5.24	86.4	18.8	[16]
Kunming, China	24°47' N	HCPV	9	3.11	79.7	18.9	Present work

4. Discussion

4.1. Influence on Energy Conversion by Environmental Parameters

The above results indicate a large variation in the performance of the HCPV system due to the changes in environmental parameters in different months. The output power of the HCPV module (P_{mod}) is expected to be mainly influenced by the intensity of DNI, temperature of the solar cell (T_{cell}) and spatial distribution of the DNI (S_b), according to ref [16], which has been described as $P_{mod} = (P^*/DNI^*)DNI[1-\delta(T_{cell}-T_{cell}^*)]S_b$, where P^* , DNI^* and T_{cell}^* are the maximum power, direct normal irradiance and cell temperature at reference conditions, while δ is the cell temperature coefficient. The spatial distribution of DNI may also influence the performance of the present HCPV system. The spatial distribution of DNI is associated with parameters such as air mass (AM), aerosol optical depth (AOD) and precipitable water (PW), since they influence the scattering of the incident sunlight with a specific wavelength [17].

The DNI is expected to be the most important environmental parameter that directly determines the output power as well as the energy generation amount. This can be also seen from the present investigation, where a much larger final yield has been observed during the dry season than the wet season due to the larger amount of DNI. By exploring their quantified correlations between the energy output of the HCPV system and the condition of direct normal irradiation for the present investigation, it is possible to forecast the energy output when applying the present HCPV technology in other regions. For a long-term forecast, the daily averaged energy output from the HCPV system is plotted as a function of the daily of direct normal radiation, as shown in Figure 3a. With an increasing amount of the daily direct normal irradiation, an approximate linear increase in the daily average energy output by the HCPV system is observed (as $E_{output} = 7.36 \times I_{DNI} - 1.03$). This quantified

correlation makes it possible to forecast the daily final energy production when constructing the present HCPV system in other regions. As a typical example, Figure 3b shows the final yield when applying the present HCPV technology at different locations of China, according to the annual direct normal irradiation distribution in China. Due to a higher direct normal irradiation, a larger final yield will be obtained when construct the present HCPV system in the northwest regions of China as compared to the southeast ones. The most favorable regions to construct the HCPV power plants are the Tibet, followed by Qinghai and Inner Mongolia.

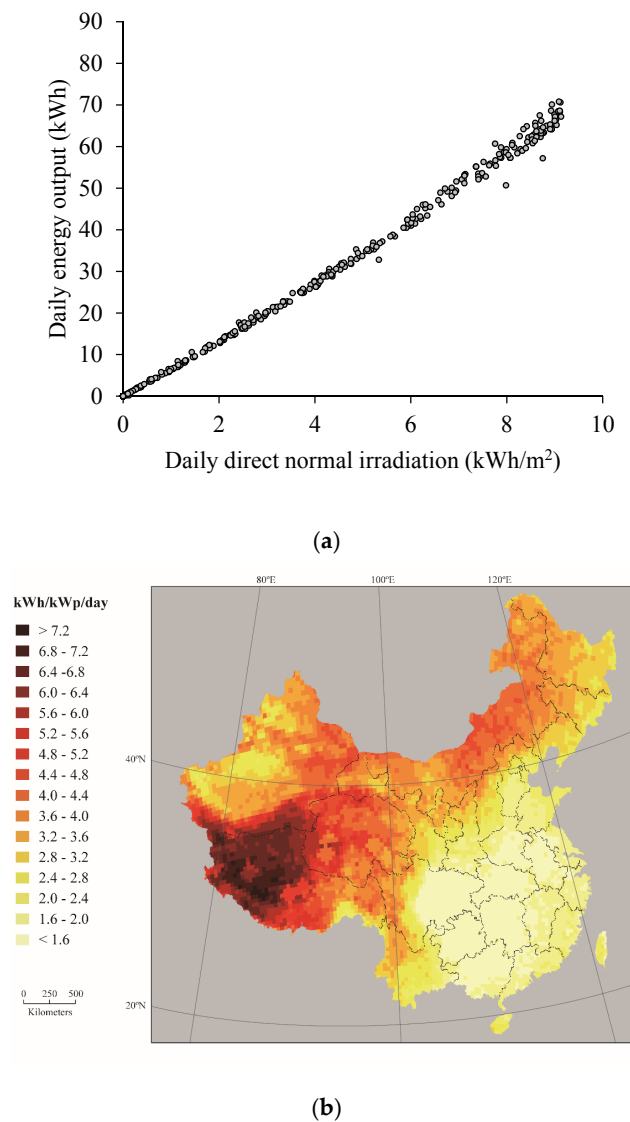
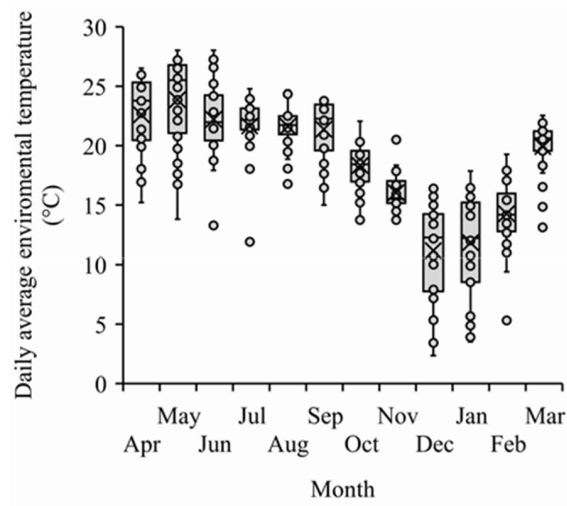
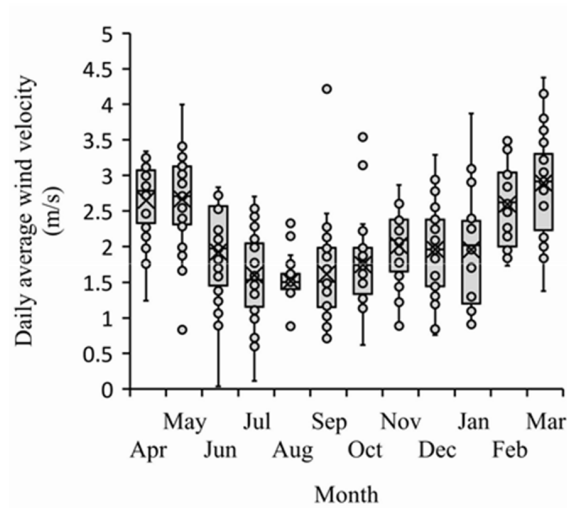


Figure 3. (a) Daily energy output plotted as a function of the daily direct normal irradiation during a whole year; (b) Estimation of the final yield when applying the present HCPV technique in China based on the performance of the present HCPV system in this investigation.

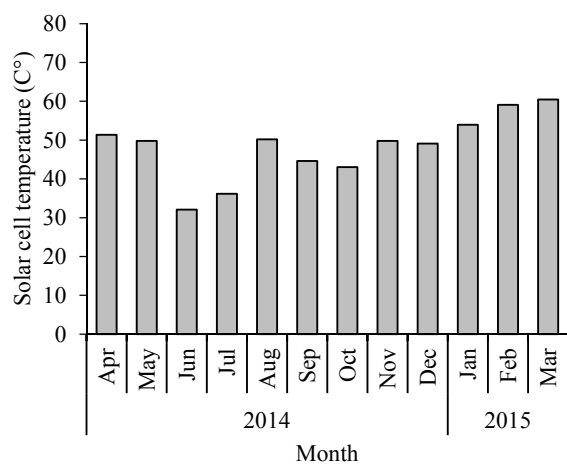
Apart from DNI, the cell temperature T_{cell} has considered to be an important parameter, since it greatly influences the conversion efficiency of the solar cell and further the performance ratio of the HCPV system. T_{cell} can be roughly estimated using the correlation given by [18] as $T_{cell} = T_{air} + aDNI + bW_s$, where T_{air} and W_s represent for air temperature and wind velocity, respectively, while a and b are constant ($a = 0.059$; $b = -2.21$). Figure 4a,b show the monthly averaged environmental temperature and wind velocity, respectively, during the operation time. Accordingly, the monthly averaged T_{cell} has been estimated and further shown in Figure 4c for different months.



(a)



(b)



(c)

Figure 4. (a) Box diagram of daily average environmental temperature during HCPV running time; (b) Box diagram of daily averaged wind velocity during HCPV running time; (c) Monthly averaged solar cell temperature.

Although possessing a lower environmental temperature, the dry season (in winter) shows a larger T_{air} than the wet season, due to a larger contribution from the DNI. For example, the highest T_{cell} observed in March is expected to result in a reduced system efficiency for about 3.4% ($\delta = 0.12$ [18]) as compared to June when the lowest T_{cell} has been observed. The above estimations are in contrast to the experimental observations that the performance ratio is observed to be higher in the dry season (March: 80.2%) than the wet season (June: 75.6%) and the system efficiency is higher in March (19.03%) as compared to June (17.94%). This indicates that in the present investigation, T_{cell} is not the direct reason for the observed larger performance ratio or system conversion efficiency of the HCPV system during the dry season as compared to the wet season. This could be related to the effective heat radiation part that maintains a relatively low T_{cell} (below 60 °C) even at the highest DNI intensity and environmental temperature, which prevents the dramatic reduction in the performance of the solar cell chip. The local AOD is not expected to have a significant change since the HCPV system is built in the remote region of Kunming. In contrast, the PW is more likely to be associated with the lower performance ratio observed for the wet season. Since water vapor possesses absorption bands in the visible and near infrared parts of the solar spectrum, the increased water vapor during cloudy days may change the distribution of light wavelength of the irradiant solar spectrum [16,17]. This will further cause the mismatches in the photocurrent generated in different junctions of the solar cell and reduces the conversion efficiency of the solar cell. Nevertheless, due to a lack of information on the AOD data for the local area, the influence from PW to the performance of the HCPV system cannot be quantified for the present case. The present investigation also shows that the HCPV module efficiency linearly reduces with an increasing air mass when $AM > 2$, while the influence of air mass can be considered negligible when $AM < 2$, which is in agreement with the previous reports [16,31].

4.2. Influence on Power Inversion by Environmental Parameters

Although the previous discussions mainly focus on the photon-to-electron energy conversion process, it is undeniable that the environmental parameters (such as DNI level) may also indirectly influence the performance of the inverter. Figure 5a shows the efficiency of the inverter related to the DNI. A dramatic decrease in η_{inv} has been observed when the DNI is around 150 W/m². This can be also seen from the relationship between the output power and DNI as shown by Figure 5b. When the intensity of DNI is below ~150 W/m², there is nearly no power output from the HCPV system due to the dramatically reduced efficiency of the inverter. At a higher intensity of DNI, a linear correlation has been roughly observed between the output power and DNI. Above result indicates that the weak DNI is not effectively utilized by the present HCPV system due to a dramatically reduced efficiency of the inverter. Figure 5c shows the monthly averaged proportion of time when the intensity DNI is lower than 150 W/m² during the daytime period. A larger proportion of low DNI level period has been observed for the wet season as compared to the dry season. This is partially the reason for the less efficient energy conversion during the wet season than the dry season.

In addition, a frequent shut-down and restart of the inverter may also result in energy generation losses. When the DNI intensity is so low that the input DC voltage is lower than 250 V, the inverter will shut down and the restarting delay is 60 seconds. This delay time is set for the inverter to perform a self-adjustment process in order to protect the public power grid and meanwhile seek the optimum working conditions. The delayed restarting of the inverter will result in the losses in capturing the solar irradiation. As a typical example, Figure A2 shows the temporal dependence in the DNI and the output power of the HCPV system measured during a typical day in the wet season. The DNI shows a large fluctuation due to the frequent shielding by the cloud, and the inverter restart for several times during one hour. A delayed power output by the HCPV system has been always observed with respective to the variation of the DNI. Figure 5d summarizes the times for restarting the inverter on average during one day for different months. A more frequent restarting of the inverter has been observed during a typical day in the wet season as compared to the dry season, which is estimated to reduce the performance ratio by up to 2.5%.

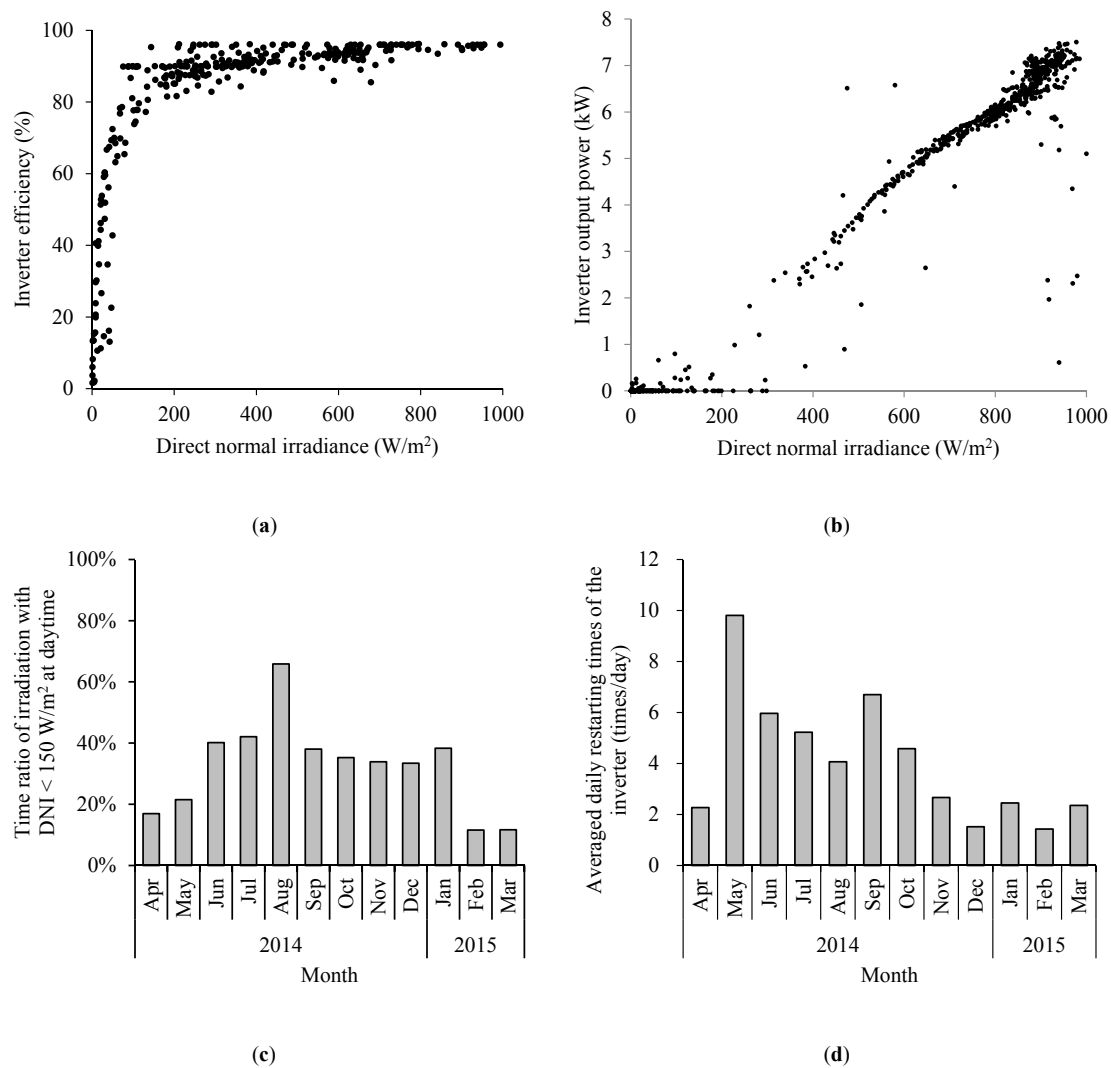


Figure 5. (a) Efficiency of the inverter plotted as a function of direct normal irradiance; (b) Output power of the inverter plotted as a function of the direct normal irradiance during a typical day; (c) Monthly proportion of time when DNI < 150 W/m² during the daytime period; (d) Monthly averaged daily restarting times of the inverter.

5. Conclusions

In conclusion, the performance of 9 kW_p HCPV system constructed in Kunming has been monitored along with the environmental parameters during different months for a period of an entire year. The amount of energy generation of the HCPV system is found to be mainly determined by the direct normal irradiation. In addition, a larger performance ratio (or system efficiency) is observed for the dry season as compared to the wet season, which is mainly associated to the power inversion process rather than the influence from cell temperature. This result indicates that apart from a direct impact on the energy conversion process of the solar cell modules, the environmental parameters have been also shown to influence the power inversion process that indirectly affects the performance of the HCPV system. The quantified correlation between the output energy by the HCPV power plant and the condition of direct normal irradiance has been further derived, which provides guidelines for both the cogent application and simulation modelling of the HCPV systems.

Acknowledgments: The authors gratefully acknowledge the financial support from the Fundamental Research Funds for the Central Universities (No. 0650027 and No. 13ZD05), the natural science foundation of Beijing (No. 2151004); National Basic Research Program of China (973-program) under Project No. 2013CB632501;

National High Technology Research and Development Program of China (Grant No. 2011AA050507), the National Natural Science Foundation of China (Grant No. 61006050).

Author Contributions: Zhe Mi and Nuofu Chen conceived and designed the experiments; Zhe Mi and Jikun Chen analyzed the data and wrote the paper; Wenwang Wu contributed analysis tools; Rui Fu and Hu Liu performed the experiments.

Conflicts of Interest: The authors declare no conflict of interest.

Appendix

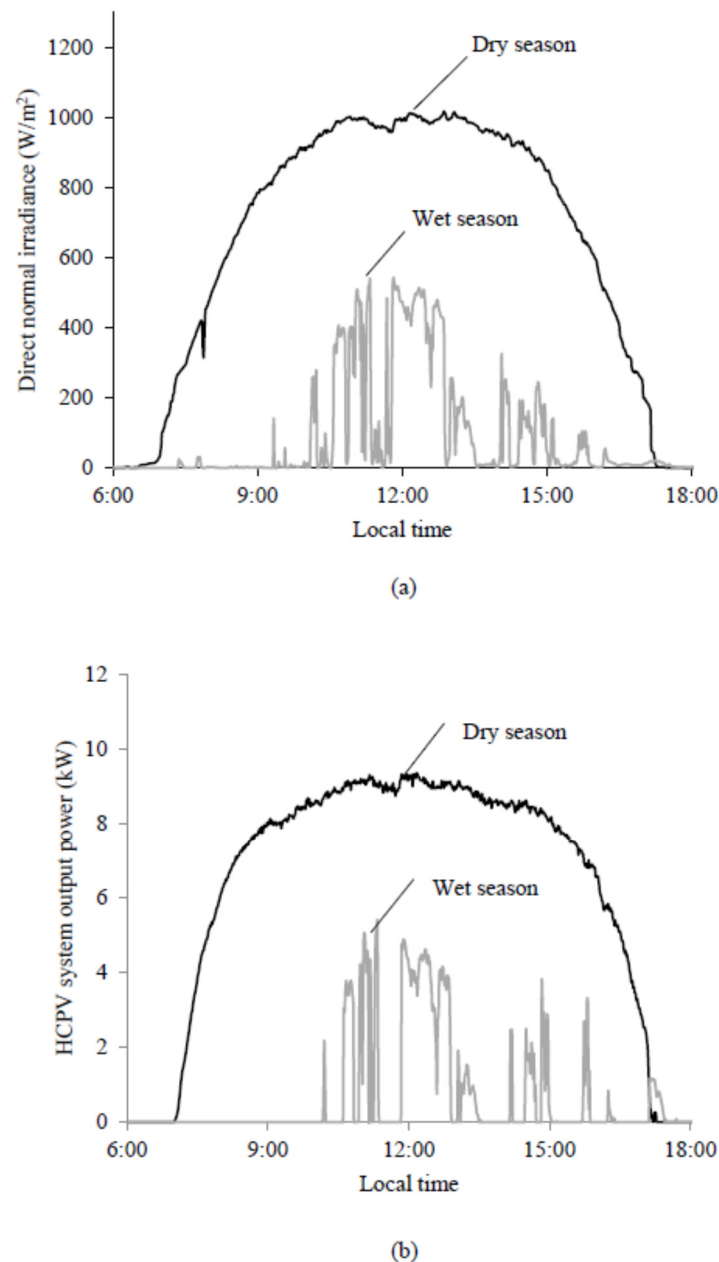


Figure A1. Dependence of HCPV output power on the direct normal irradiance in typical days of the dry season (21 February 2015) and wet season (6 June 2014): (a) Direct normal irradiance; (b) HCPV system output power.

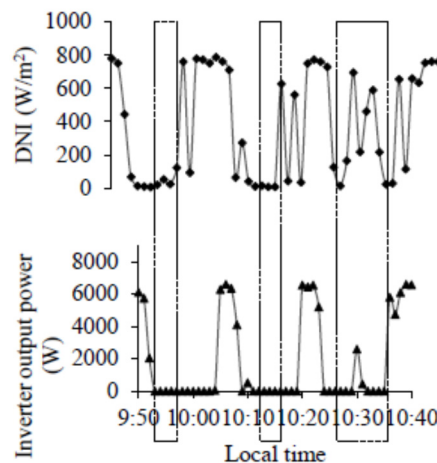


Figure A2. Comparison of the DNI and output power of the HCPV system measured at a typical period of time in wet season (11 September 2014).

References

1. Ren, P.S. *Renewables 2015 Global Status Report*; REN21 Secretariat: Paris, France, 2015.
2. Foresi, J.; Babej, A.; Han, R.; Liao, T.; Wang, C. Characterization of Suncore's utility-scale CPV power plants. In Proceedings of the 11st International Conference on Concentrator Photovoltaic Systems: CPV-11, Aix-les-Bains, France, 17 March 2015.
3. Gerstmaier, T.; Zech, T.; Röttger, M.; Braun, C.; Gombert, A. Large-scale and long-term CPV power plant field results. In Proceedings of the 11st International Conference on Concentrator Photovoltaic Systems: CPV-11, Aix-les-Bains, France, 17 March 2015.
4. Talavera, D.L.; Pérez-Higueras, P.; Ruíz-Arias, J.A.; Fernández, E.F. Levelised cost of electricity in high concentrated photovoltaic grid connected systems: Spatial analysis of Spain. *Appl. Energy* **2015**, *151*, 49–59. [[CrossRef](#)]
5. Xie, W.T.; Dai, Y.J.; Wang, R.Z.; Sumathy, K. Concentrated solar energy applications using Fresnel lenses: A review. *Renew. Sustain. Energy Rev.* **2011**, *15*, 2588–2606. [[CrossRef](#)]
6. Miller, D.C.; Kurtz, S.R. Durability of Fresnel lenses: A review specific to the concentrating photovoltaic application. *Sol. Energy Mater. Sol. Cells* **2011**, *95*, 2037–2068. [[CrossRef](#)]
7. Fraunhofer ISE New World Record for Solar Cell Efficiency at 46% French-German Cooperation Confirms Competitive Advantage of European Photovoltaic Industry. Available online: <http://www.ise.fraunhofer.de/en/press-and-media/press-releases/press-releases-2014/new-world-record-for-solar-cell-efficiency-at-46-percent> (accessed on 9 August 2015).
8. Araki, K. Performance of the 30 kW CPV system installed in coastal area in Japan. In Proceedings of the 6th International Conference on Concentrating Photovoltaic Systems: CPV-6, Freiburg, Germany, 7–9 April 2010.
9. Gómez-Gil, F.J.; Wang, X.; Barnett, A.; Gómez-Gil, F.J.; Wang, X. Analysis and prediction of energy production in concentrating photovoltaic (CPV) installations. *Energies* **2012**, *5*, 770–789. [[CrossRef](#)]
10. Terao, A.; Mulligan, W.P.; Daroczi, S.G.; Pujol, Ò.C.; Verlinden, P.J.; Swanson, R.M.; Minano, J.C.; Benitz, P.; Álvarez, J.L. A mirror-less design for micro-concentrator modules. In Proceedings of the Twenty-Eighth IEEE Photovoltaic Specialists Conference, Anchorage, AK, USA, 15–22 September 2000; pp. 1416–1419.
11. Han, Y.M.; Wang, R.Z.; Dai, Y.J.; Xiong, A.H. Studies on the light permeance characteristic of a Fresnel lens group applied in high concentration solar energy. *J. Opt. A Pure Appl. Opt.* **2007**, *9*, 988–997. [[CrossRef](#)]
12. Mousazadeh, H.; Keyhani, A.; Javadi, A.; Mobli, H.; Abrinia, K.; Sharifi, A. A review of principle and sun-tracking methods for maximizing solar systems output. *Renew. Sustain. Energy Rev.* **2009**, *13*, 1800–1818. [[CrossRef](#)]
13. Zhang, Q.X.; Yu, H.Y.; Zhang, Q.Y.; Zhang, Z.Y.; Shao, C.H.; Yang, D. A solar automatic tracking system that generates power for lighting greenhouses. *Energies* **2015**, *8*, 7367–7380. [[CrossRef](#)]

14. Bird, R.; Riordan, C. Simple solar spectral model for direct and diffuse irradiance on horizontal and tilted planes at the earth's surface for cloudless atmospheres. *J. Appl. Meteorol.* **1986**, *25*, 87–97. [[CrossRef](#)]
15. Perez, R.; Seals, R.; Ineichen, P.; Stewart, R.; Menicucci, D. A new simplified version of the perez diffuse irradiance model for tilted surfaces. *Sol. Energy* **1987**, *39*, 221–231. [[CrossRef](#)]
16. Fernández, E.F.; Pérez-Higueras, P.; Almonacid, F.; Ruiz-Arias, J.A.; Rodrigo, P.; Fernandez, J.I.; Luque-Heredia, I. Model for estimating the energy yield of a high concentrator photovoltaic system. *Energy* **2015**, *87*, 77–85. [[CrossRef](#)]
17. Chan, N.L.A.; Brindley, H.E.; John, E.D.N. Impact of individual atmospheric parameters on CPV system power, energy yield and cost of energy. *Prog. Photovolt. Res. Appl.* **2013**, *22*, 1080–1095. [[CrossRef](#)]
18. Almonacid, F.; Pérez-Higueras, P.J.; Fernández, E.F.; Rodrigo, P. Relation between the cell temperature of a HCPV module and atmospheric parameters. *Sol. Energy Mater. Sol. Cells* **2012**, *105*, 322–327. [[CrossRef](#)]
19. Or, A.B.; Appelbaum, J. Dependence of multi-junction solar cells parameters on concentration and temperature. *Sol. Energy Mater. Sol. Cells* **2014**, *130*, 234–240.
20. CWA Space Distribution of Global Horizontal Radiation from 1978 to 2007 in China. Available online: <http://cwera.cma.gov.cn/Website/index.php?ChannelID=121&NewsID=1988> (accessed on 10 August 2014).
21. Bai, Y. GaAs Based Solar Cells and Key Problems in Concentrators. Ph.D. Thesis, Chinese Academy Sciences, Beijing, China, 2007.
22. International Electrotechnical Commission (IEC). *Photovoltaic System Performance Monitoring—Guidelines for Measurement, Data Exchange and Analysis*; IEC Standard 61724; IEC: Geneva, Switzerland, 1998.
23. Okello, D.; van Dyk, E.E.; Vorster, F.J. Analysis of measured and simulated performance data of a 3.2 kW_p grid-connected PV system in Port Elizabeth, South Africa. *Energy Convers. Manag.* **2015**, *100*, 10–15.
24. Ghiani, E.; Pilo, F.; Cossu, S. Evaluation of photovoltaic installations performances in Sardinia. *Energy Convers. Manag.* **2013**, *76*, 1134–1142. [[CrossRef](#)]
25. King, B.; Riley, D.; Hansen, C.; Erdman, M.; Gabriel, J.; Ghosal, K. HCPV characterization: Analysis of fielded system data. In Proceedings of the AIP 2014: Australian Institute of Physics Congress, Canberra, Australia, 7–12 December 2014; pp. 276–279.
26. Wu, X.; Liu, Y.; Xu, J.; Lei, W.; Si, X.; Du, W.; Zhao, C.; Zhong, Y.; Peng, L.; Lin, J. Monitoring the performance of the building attached photovoltaic (BAPV) system in Shanghai. *Energy Build.* **2015**, *88*, 174–182. [[CrossRef](#)]
27. Ayompe, L.M.; Duffy, A.; McCormack, S.J.; Conlon, M. Measured performance of a 1.72 kW rooftop grid connected photovoltaic system in Ireland. *Energy Convers. Manag.* **2011**, *52*, 816–825.
28. Pu, S.; Lin, W. Correlations to estimate monthly total solar radiation on horizontal surfaces at Kunming, China. *Energy Convers. Manag.* **2000**, *41*, 367–374. [[CrossRef](#)]
29. Tripathi, B.; Yadav, P.; Rathod, S.; Kumar, M. Performance analysis and comparison of two silicon material based photovoltaic technologies under actual climatic conditions in Western India. *Energy Convers. Manag.* **2014**, *80*, 97–102. [[CrossRef](#)]
30. Al-Otaibi, A.; Al-Qattan, A.; Fairouz, F.; Al-Mulla, A. Performance evaluation of photovoltaic systems on Kuwaiti schools' rooftop. *Energy Convers. Manag.* **2015**, *95*, 110–119. [[CrossRef](#)]
31. Fernández, E.F.; Pérez-Higueras, P.; Almonacid, F.; García Loureiro, A.J.; Fernández, J.I.; Rodrigo, P.; Vidal, P.G.; Almonacid, G. Quantifying the effect of air temperature in CPV modules under outdoor conditions. In Proceedings of the 8th International Conference on Concentrating Photovoltaic Systems, Toledo, Spain, 16–18 April 2012; pp. 194–197.

